Ultrasonic evaluation of early damage of a coating by using second-harmonic generation technique

Guoshuang Shui[a] and Yue-Sheng Wang[b]
Department of Engineering Mechanics, Beijing Jiaotong University, Beijing 100044, China

(Received 14 January 2012; accepted 12 May 2012; published online 19 June 2012)

For an in-service structure with a coating, damage accumulation may develop gradually within the coating or at the interface between the substrate and coating under external loads. By considering the fact that different levels of external load are closely related to the degrees of accumulated early damage which is very difficult to be measured directly, and that the early damage may cause the nonlinearity of Rayleigh surface waves, the acoustic nonlinearity parameter (ANP) is employed as an indicator of early damage of a coating. This research reports on the experimental observation of the monotonic correlation between the ANP measured with nonlinear Rayleigh waves and the applied stress on an AZ31 magnesium alloy plate specimen using ultrasonic second-harmonic generation technique. Rayleigh waves are generated and detected with wedge transducers, and the nonlinearity parameters are measured at different stress levels for the specimens with coatings. The result shows that there is a significant increase in the nonlinearity parameters with the increasing tensile stress although there is no obvious change for the coating when the tensile stress is less than a certain level. The research suggests an effective nondestructive evaluation method to track the coating damage using the higher order harmonic generation technique. © *2012 American Institute of Physics*. [http://dx.doi.org/10.1063/1.4729300]

I. INTRODUCTION

Recently, the second-harmonic generation (SHG, also known as nonlinear ultrasonics) technique has been emerging as a potential non-destructive evaluation (NDE) tool for the assessment of the mechanical properties degradation.[1–9] In this technique, high amplitude ultrasonic waves of a particular frequency are excited to propagate through the material. The harmonics generated due to the interaction of ultrasonic waves with the microstructures are detected and the amplitudes of the harmonics are used for the assessment of the mechanical properties degradation. The ratio of the second harmonic amplitude to that of the square of the fundamental amplitude, known as the acoustic nonlinearity parameter (ANP), is determined and used for material characterization.

The second-harmonic wave is more sensitive to the micro-damage than the conventional linear ultrasonic wave. Hikata *et al.*[10] carried out theoretical and experimental studies in aluminum single crystals subjected to an external bias stress and established a dependence of ANP on dislocation density and dislocation loop length. Frouin *et al.*[11] used the SHG technique to detect the early fatigue damage in Ti–6Al–4V specimens. They reported that the ANP significantly increases with the increase in the number of fatigue cycles. Jhang and Kim[12] studied the material degradation in steel SS 41 and SS 45 during stretch loading using SHG and reported that ANP increases with degree of deformation. Deng and Pei[13] assessed the accumulated fatigue damage in solid plates using nonlinear Lamb wave approach. Pruell *et al.*[14] analyzed the effect of plastic deformation in Al 1100-H16 alloy and reported that the residual stress arising due to the statically induced plastic strain will increase the ANP. Sagar *et al.*[15] studied the effect of the microstructure on non-linear behavior of ultrasound during low cycle fatigue of pearlitic steels and concluded that the non-linear parameter follows the fatigue hardening and softening trends in this steel.

Nonlinear Rayleigh wave is also effectively used to for material surface characterization in recent years. Compared with bulk waves used in the SHG technique, Rayleigh surface waves have some advantages. For instance, Rayleigh waves do not require access to both sides of a component; most of the energy of Rayleigh waves is concentrated near the surface, which can lead to stronger nonlinear effects; and Rayleigh waves can propagate a far distance, making them an ideal mean to interrogate large, complex components. Recent examples of using nonlinear Rayleigh waves include measuring residual stress in shot-peened aluminum plates,[16] assessment of material damage in a nickel based superalloy,[17] and measurement of material nonlinearity by using surface acoustic wave parametric interaction and laser ultrasonics.[18] Shui *et al.* measured the ANP of aluminum alloy plate specimens which underwent no loading[19] and characterized the surface damage of a solid plate under tensile loading by using Rayleigh waves.[20]

Coatings are more and more widely used in aircrafts, aeronautics, and microelectro-mechanical systems. In many cases, coatings are applied to improve surface properties of materials, such as appearance, adhesion, corrosion resistance, wear resistance, and scratch resistance. It is necessary to evaluate the characteristics of thin coating layers nondestructively for reliable use of coated components. For an in-service structure with a coating, damage accumulation may develop gradually within the coating or at the interface

[a]Author to whom correspondence should be addressed. Electronic mail: gsshui@bjtu.edu.cn.
[b]yswang@bjtu.edu.cn.

between the substrate and coating. Although direct measurement of this early damage is very difficult, the damage may cause the nonlinearity of ultrasonic waves, particularly of Rayleigh surface waves propagating along the material surface as mentioned above. It is, therefore, possible to evaluate the early damage of the coating using the nonlinearity of Rayleigh waves. Until now, characterization of a coating is mainly based on conventional nondestructive evaluation techniques by employing the linear properties of acoustic waves. For example, Wang *et al.*[21] characterized the adhesive bonds between an epoxy coating and an aluminum substrate by establishing the relation between the interfacial stiffness and the amplitude ratio of the reflected and direct waves; Kim *et al.*[22] evaluated the bonding quality of chemical vapor deposit diamond coating layers having different bonding conditions by measuring energy of reflected Rayleigh-like waves with variation of the incidence angle from normal to beyond Rayleigh angle in a pitch-catch immersion setup; Kramb *et al.*[23] correlated the microscopic images obtained using the NDE methods with the measured physical and chemical changes for weathering degradation in aircraft polymeric coatings. As far as we know, attempts to apply the SHG technique to nondestructively evaluate the early damage of a coating have not been reported. In this research, an experimental technique for the ultrasonic evaluation of coating damage based on the SHG technique is developed by measuring of the relative ANP of coated materials under tensile loading using nonlinear Rayleigh surface waves. The specimens with coatings are loaded to different stresses, which will lead to accumulated damage at different levels corresponding to respective stresses. On condition that the damage variables cannot be measured directly, the relation between the ANP and stress, instead of the damage variable, is established. In fact, this relation is of practical importance in engineering because the degree of damage accumulation is closely related to the stress levels.

II. DEVELOPMENT OF NONLINEAR PARAMETER FOR RAYLEIGH SURFACE WAVES

A. ANP

Considering that a Rayleigh surface wave propagates in the positive x-direction. The z-axis points into the material half-space (Fig. 1). The displacement potentials that describe the longitudinal and shear waves are written as[24]

$$\varphi = -i\frac{B_1}{k_R}e^{-pz}e^{i(k_Rx-\omega t)}, \quad \psi = -i\frac{C_1}{k_R}e^{-sz}e^{i(k_Rx-\omega t)}, \tag{1}$$

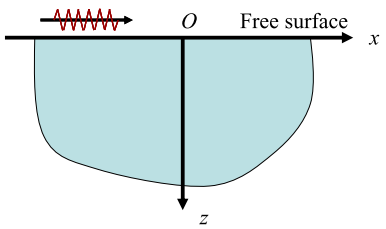

FIG. 1. Free surface half space and the coordinate system.

where $p^2 = k_R^2 - k_l^2$; $s^2 = k_R^2 - k_s^2$; and k_R, k_l, and k_s are wave numbers for the Rayleigh, longitudinal, and shear waves, respectively. Applying the stress free boundary conditions on the surface leads to following relationship for the constants B_1 and C_1 in Eq. (1)

$$B_1 = -i\frac{2k_Rp}{k_R^2+s^2}C_1. \tag{2}$$

Considering that Rayleigh waves are the superposition of inhomogeneous longitudinal and shear waves that propagate along a stress free surface having the same trace velocity, we can decompose the displacement components into their longitudinal and shear contributions,

$$u_x = B_1\left(e^{-pz} - \frac{2ps}{k_R^2+s^2}e^{-sz}\right)e^{i(k_Rx-\omega t)}, \tag{3}$$

$$u_z = iB_1\frac{p}{k_R}\left(e^{-pz} - \frac{2k_R^2}{k_R^2+s^2}e^{-sz}\right)e^{i(k_Rx-\omega t)}. \tag{4}$$

In a medium having a weak quadratic nonlinearity, the second harmonic Rayleigh waves propagating a sufficiently large distance can be written as[25]

$$u_x \approx B_2\left(e^{-2pz} - \frac{2ps}{k_R^2+s^2}e^{-2sz}\right)e^{i2(k_Rx-\omega t)}, \tag{5}$$

$$u_z \approx iB_2\frac{p}{k_R}\left(e^{-2pz} - \frac{2k_R^2}{k_R^2+s^2}e^{-2sz}\right)e^{i2(k_Rx-\omega t)}. \tag{6}$$

The acoustic nonlinearity for the shear wave in an isotropic material vanishes due to the symmetry of the third order elastic constants.[26,27] The amplitudes of the in-plane displacement (u_x) of the fundamental and second harmonics, therefore, can be related to those in the bulk longitudinal waves, that is,

$$B_2 = \frac{\beta k_l^2 x B_1^2}{8}, \tag{7}$$

where β is the acoustic nonlinearity parameter for the longitudinal waves, and x is the propagation distance. From Eqs. (4), (6), and (7), the ratio of the second harmonic amplitude to the fundamental amplitude is

$$\frac{u_z(2\omega;x,0)}{u_z^2(\omega;x,0)} \approx \frac{\beta k_l^2 x}{8i(p/k_R)\left(1-\frac{2k_R^2}{k_R^2+s^2}\right)}, \tag{8}$$

where $u_z(\omega,x,0)$ and $u_z(2\omega,x,0)$ are the vertical components of the particle displacements on the surface ($z=0$) for the fundamental and second-harmonic frequencies, respectively. The measured out-of-plane displacement components, therefore, are related to the ANP

$$\beta = \frac{u_z(2\omega;x,0)}{u_z^2(\omega;x,0)}\frac{8i}{k_l^2x}\frac{p}{k_R}\left(1-\frac{2k_R^2}{k_R^2+s^2}\right). \tag{9}$$

B. Stress wave factor based acoustic nonlinearity parameter (SWF-based ANP)

Note that the ANP in Eq. (9) is based on a fixed exciting frequency. In order to know more about the relation between the material surface plastic damage and the ultrasonic harmonics (fundamental and second harmonics), further experimental tests were conducted to get the normalized nonlinearity parameter with different exciting signal frequencies. The received ultrasonic Rayleigh wave signal can be assumed as a time-domain burst $F(t)$, modulated by a term $A_r(t)$. $F(t)$ can thus be written as

$$F(t) = A_r(t)\sin(2\pi f_r t + \varphi_r), \tag{10}$$

where φ_r is the phase shift in the transducer and specimen, including the effect of the Rayleigh wave propagation time. The carrier frequency f_r equals f (for the fundamental harmonic) or $2f$ (for the second harmonic). The Ritec-SNAP system processes two integration signals associated with $A_r(t)$

$$I_1 = C\cos\varphi_r \int_{t_1}^{t_2} A_r(t)dt, \quad I_2 = C\sin\varphi_r \int_{t_1}^{t_2} A_r(t)dt, \tag{11}$$

where $A_r(t)$ is located between t_1 and t_2 (Fig. 2); and C is a constant associated with the parameter setups of the Ritec-SNAP system.

Denote

$$\bar{A}_r(f_r) = \int_{t_1}^{t_2} A_r(t)dt = \frac{1}{C}\sqrt{I_1^2 + I_2^2} \tag{12}$$

then a parameter, which includes the influences of the various frequencies is defined as[28]

$$\mathrm{SWF}(f_r) = \int_{f_1}^{f_2} \bar{A}_r(f_r)df. \tag{13}$$

This parameter is named as SWF. All the features of Rayleigh waves associated with the surface properties are reflected by the parameter SWF(f_r). It is, therefore, reasonable to use SWF(f_r) to characterize the changes of the surface properties. Define an SWF-based nonlinearity parameter (SWF-based ANP) as

$$\beta_R'^{SWF} = \frac{\mathrm{SWF}(2f)}{[\mathrm{SWF}(f)]^2}. \tag{14}$$

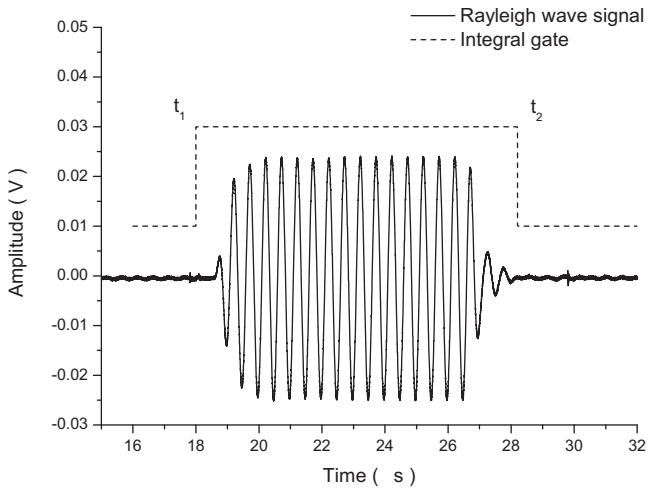

FIG. 2. Rayleigh wave signal and the integral zone.

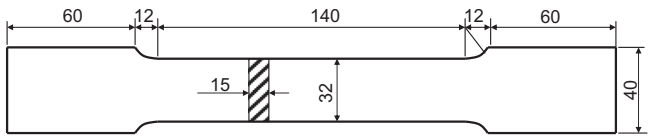

FIG. 3. Dimension of AZ31 magnesium-aluminum alloy specimen with nickel coating (unit: mm).

III. EXPERIMENTAL SETUP

Dimension of the specimen for tensile stretch testing was shown in Fig. 3. In this study, the dog-bone specimens for tensile stretch testing are made of AZ31 magnesium-aluminum alloy, with the yielding stress 199 MPa, elastic modulus 46 GPa, Poisson's ratio 0.27, and density 1770 kg/m^3. The specimens were prepared by electroplating method with nickel coating. The thickness of the coating is about 0.3–0.5 mm, which is less than a quarter of the wave length of Rayleigh waves. During the experimental measurements, five specimens were selected, and they were loaded to different loading levels, and then unloaded, respectively. The ultrasonic measurements were performed on the unloaded specimen at a fixed propagation distance. The same procedure was repeated for increasing maximum loads until the tensile stress reached 150 MPa when discernable damage was observed. Figs. 4(a) and 4(b) show the appearance of the nickel coating when the stress is less than and near 150 MPa, respectively. Obvious change can be observed when the tensile stress is near 150 MPa, see Fig. 4(b).

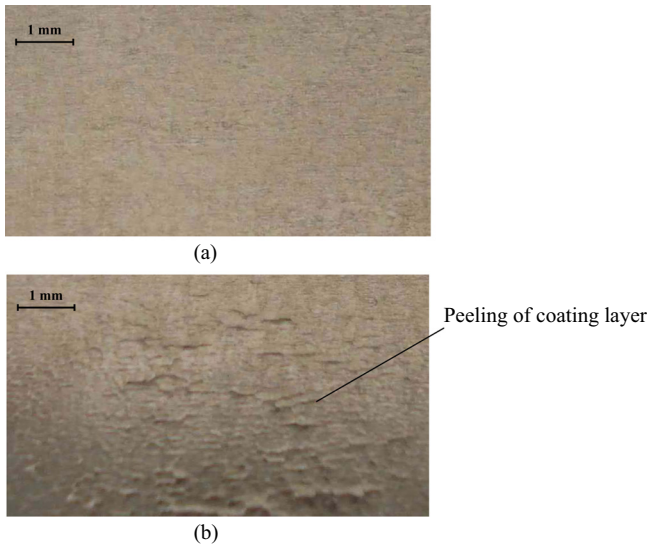

FIG. 4. Illustration of the change of nickel coating (a) without obvious change when the stress is less than 150 MPa, and (b) with local obvious change when the stress is near 150 MPa.

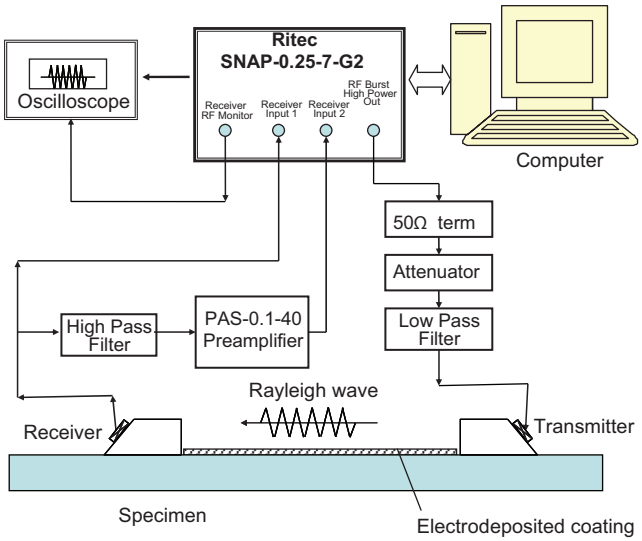

FIG. 5. Experimental setup of evaluating the degradation of a coating by using Rayleigh waves.

A schematic diagram for the experimental setup is shown in Fig. 5. The transmitting wedge transducer (T) was driven by a tone burst signal of 16 cycles at 2 MHz. The receiving wedge transducer (R) was used to detect the fundamental and second harmonics of Rayleigh waves. The wedge angle is 65°. The central frequencies of T and R are, respectively, 2 MHz and 4 MHz. The tone burst signal was generated by Ritec SNAP-0.25-7-G2 nonlinear measurement system with the high-power gated amplifier. Before driving the transmitting wedge transducer, the high voltage signal passed through a 50 Ω termination, an attenuator and a set of low-pass filter so that the transient behavior and high frequency component from the amplifier were suppressed. Fig. 6 presents the amplitude–frequency curves of the low-pass and high-pass filters. Compared with similar instruments available, this nonlinear measurement system can provide a more monochromatic ultrasonic sine wave signal with higher quality, and this will decrease the acoustic nonlinearity from the signal as less as possible.

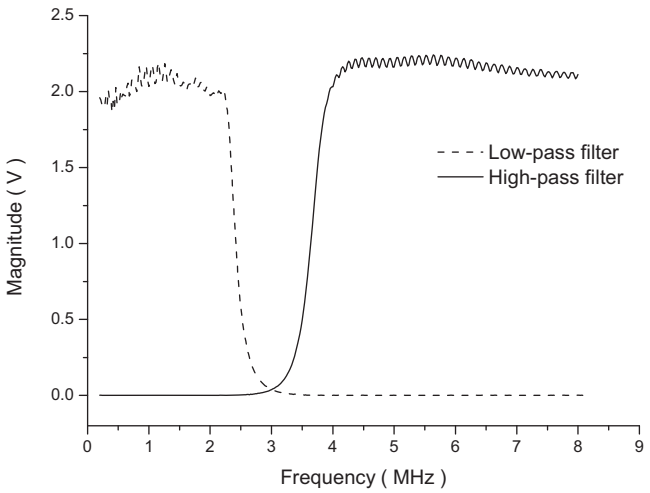

FIG. 6. Magnitude as a function of frequency for low-pass and high-pass filter.

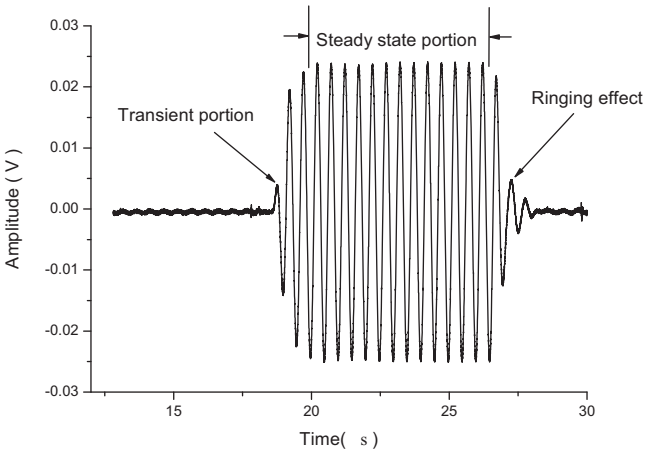

FIG. 7. Received nonlinear ultrasonic Rayleigh waves.

A typical Rayleigh wave signal, generated and detected by the wedge transducers (with propagation distance of 100 mm), is shown in Fig. 7. The sampling rate of oscilloscope is 1.25 GS/s. The signal of entire length consists of a transient part at the beginning, a steady state portion, and finally the turnoff ringing at the end. To make sure that only the steady-state part of the tone burst signal was used, a Hanning window was applied to the acquired time-domain signal for fast Fourier transform (FFT). Therefore, only the data points within the steady-state part were selected and then transformed to the frequency domain where the magnitudes of the fundamental and higher order harmonics of the detected Rayleigh surface waves become visible. Fig. 8 shows the magnitudes of the fundamental (A_1) and second harmonics (A_2) in the frequency domain, respectively.

In order to ensure that the measured second order harmonics are due to the material nonlinearity rather than the spurious nonlinearity from the experimental instrumentation, the input voltage for excitation of the transducer was varied to different levels with the fundamental and second harmonics being detected by using the same specimen and propagation distance. Fig. 9 shows the second harmonic amplitude (A_2) versus the square of the fundamental amplitude (A_1^2) for increasing driving voltages. A linear relationship is clearly

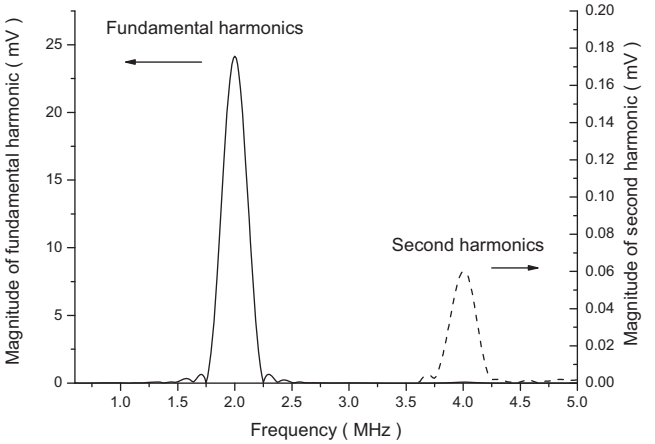

FIG. 8. Magnitudes of the fundamental and second harmonics of the Rayleigh waves.

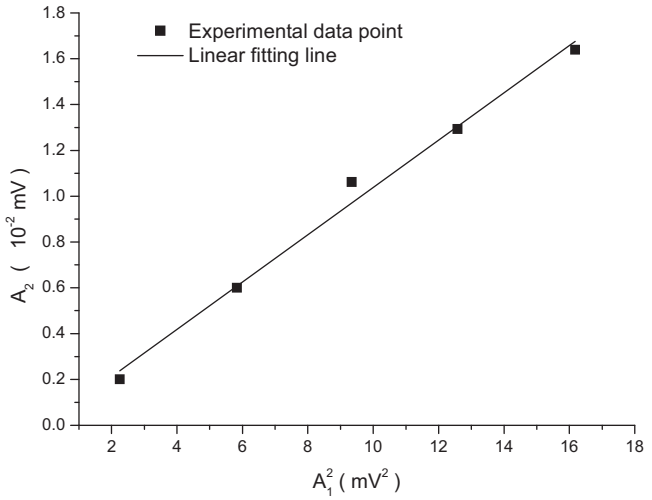

FIG. 9. Relation between the magnitude of the second and fundamental harmonics under different voltage levels.

observed for different driving voltages, which means that A_2/A_1^2 keeps constant for different voltages at a fixed propagation distance. This will make sure that the measured higher harmonics are an indicator of material nonlinearity instead of spurious nonlinearity due to the instrumentation.

IV. RESULTS AND DISCUSSION

Since $u_z(\omega)$ and $u_z(2\omega)$ in Eq. (9) are proportional to the magnitudes of the fundamental and second harmonics, A_1 and A_2, for Rayleigh waves in the frequency domain, in this measurement, we use, for convenience, a relative ANP defined as

$$\beta_R = \frac{A_2}{A_1^2}. \tag{15}$$

Clearly, this relative ANP β_R is proportional to the absolute material ANP β in Eq. (9) for a fixed propagation distance.

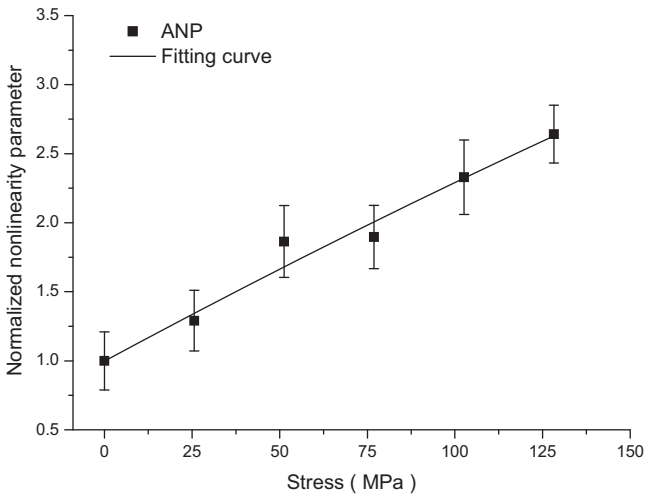

FIG. 10. Normalized relative nonlinearity parameter as a function of the stress for AZ31 magnesium-aluminum alloy with the coating by using Rayleigh waves.

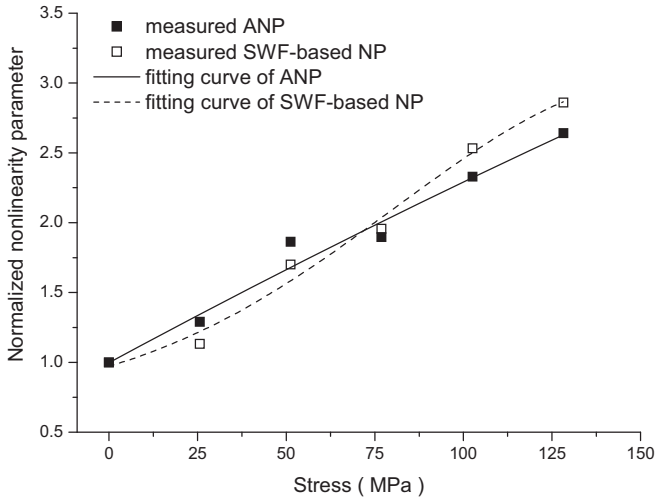

FIG. 11. Comparison of the normalized ANP and SWF-based ANP.

Fig. 10 shows the normalized relative ANP (β_N) as a function of the applied stress. Here, the normalized ANP β_N is the ratio of relative nonlinearity parameter measured in each specimen (β_R) to that measured in the specimen undergoing no initial loading (β_{R0}), i.e., $\beta_N = \beta_R/\beta_{R0}$. Existence of β_{R0} is due to the third order elastic constants or initial damage of the specimens. The error bars were obtained by repeating the ultrasonic measurements three times. Note that the transducer assembly was completely removed and reattached to the specimen edge for each measurement. It is shown in Fig. 10 that the normalized ANP β_N increases with the tensile stress, although there is no obvious change for the coating when the tensile stress is less than 150 MPa. The result shows the dependence of the acoustic nonlinearity on the plastic deformation that occurs during monotonically increasing loading.

As for the SWF-based ANP, it is also normalized by the value measured in the specimen undergoing no initial loading. Then, we illustrate the normalized SWF-based ANP (β_R^{SWF}) as a function of the applied stress in Fig. 11. It is observed that there is a monotonic relationship between β_R^{SWF} and the stress. For comparison, the measured results of the ANP based on a fixed transmitting frequency are also plotted in Fig. 10. We can see that the SWF-based ANP is a little more sensitive to the coating damage.

V. CONCLUSION

Accumulated coating damage will cause an increase in the acoustic nonlinearity measured with Rayleigh waves, which means that there is a fundamental relationship between the coating damage and acoustic nonlinearity. Because the degree of damage accumulation is closely related to the stress levels, the relation between the ANP or SWF-based ANP and the stress is established in this research. The present experimental results show that both the normalized ANP and SWF-based ANP increase with the tensile stress, although there is no obvious change for the coating when the tensile stress is less than 150 MPa. We can come to the conclusion that there is a monotonic correlation

between the acoustic nonlinearity of the coating (presented in the form of acoustic nonlinearity parameters) and its accumulated damage. Rayleigh waves, therefore, can be used to evaluate the coating damage by using the established SHG technique.

Although there are other prospective candidates, such as the magnetic method,[29] etc. for nondestructive evaluation of damage, the present SHG technique is doubtless the most prospective one. It will be important for practical structural health monitoring and life prediction applications.

ACKNOWLEDGMENTS

Supports by the National Natural Science Foundation of China (11172034) and the Fundamental Research Funds for the Central Universities (2011JBM263) are acknowledged. The second author is also grateful to the National Basic Research Program of China (973 program) (2010CB732104).

[1]D. J. Barnard, G. E. Dace, and O. Buck, J. Nondestruct. Eval. **16**, 67 (1997).
[2]P. B. Nagy, Ultrasonics **36**, 375 (1998).
[3]J. H. Cantrell, Philos. Mag. **86**, 1539 (2006).
[4]J. H. Cantrell, Proc. R. Soc. London, Ser. A **460**, 757 (2004).
[5]J. Y. Kim, L. J. Jacobs, J. Qu, and J. W. Littles, J. Acoust. Soc. Am. **120**, 1266 (2006).
[6]M. Deng, J. Appl. Phys. **94**, 4152 (2003).
[7]G. S. Shui, Y. S. Wang, and J. Qu, Adv. Mech. **35**, 52 (2005) (in Chinese).
[8]J. Qu, L. J. Jacobs, and P. B. Nagy, J. Acoust. Soc. Am. **129**, 3449 (2011).
[9]K. H. Matlack, J. Y. Kim, L. J. Jacobs, and J. Qu, J. Appl. Phys. **109**, 014905 (2011).
[10]A. Hikata, B. B. Chick, and C. Elbaum, J. Appl. Phys. **36**, 229 (1965).
[11]J. Frouin, S. Sathish, T. E. Matikas, and J. K. Na, J. Mater. Res. **14**, 1295 (1999).
[12]K. Y. Jhang and K. C. Kim, Ultrasonics **37**, 39 (1999).
[13]M. Deng and J. Pei, Appl. Phys. Lett. **90**, 121902 (2007).
[14]C. Pruell, J. Y. Kim, J. Qu, and L. J. Jacobs, Appl. Phys. Lett. **91**, 231911 (2007).
[15]S. P. Sagar, A. K. Metya, M. Ghosh, and S. Sivaprasad, Mater. Sci. Eng., A **528**, 2895 (2011).
[16]M. Liu, J. Y. Kim, L. J. Jacobs, and J. Qu, NDT & E Int. **44**, 67 (2011).
[17]J. Herrmann, J. Y. Kim, L. J. Jacobs, J. Qu, J. W. Littles, and M. F. Savage, J. Appl. Phys. **99**, 124913 (2006).
[18]T. Stratoudaki, R. Ellwood, S. Sharples, M. Clark, M. G. Somekh, and I. J. Collison, J. Acoust. Soc. Am. **129**, 1721 (2011).
[19]G. S. Shui, J. Y. Kim, J. Qu, Y. S. Wang, and L. Jacobs, NDT & E Int. **41**, 326 (2008).
[20]G. S. Shui and Y. S. Wang, Theor. Appl. Mech. Lett. **1**, 051005 (2011).
[21]H. Wang, M. L. Qian, and W. Liu, Ultrasonics **44**, e1349 (2006).
[22]H. J. Kim, S. J. Song, D. Y. Kim, and S. D. Kwon, Rev. Prog. Quant. Nondestr. Eval. **27**, 1066 (2008).
[23]V. A. Kramb, J. P. Hoffmann, and J. A. Johnson, Rev. Prog. Quant. Nondestr. Eval. **22**, 1111 (2003).
[24]I. A. Viktorov, *Rayleigh and Lamb Waves* (Plenum, New York, 1967).
[25]E. A. Zabolotskaya, J. Acoust. Soc. Am. **91**, 2569 (1992).
[26]W. A. Green, Arch. Ration. Mech. Anal. **19**, 20 (1965).
[27]A. N. Norris, J. Elast. **25**, 247 (1991).
[28]M. Deng, Ultrasonics **44**, e1157 (2006).
[29]K. Yao, B. Deng, and Z. D. Wang, NDT & E Int. **47**, 7 (2011).